The EMBO Journal (2012) 31, 150–161 | © 2012 European Molecular Biology Organization | All Rights Reserved 0261-4189/12
www.embojournal.org

THE EMBO JOURNAL

RNA/DNA hybrid binding affinity determines telomerase template-translocation efficiency

Xiaodong Qi[1,3], Mingyi Xie[1,3,4], Andrew F Brown[1,3], Christopher J Bley[1], Joshua D Podlevsky[2] and Julian J-L Chen[1,2,*]

[1]Department of Chemistry and Biochemistry, Arizona State University, Tempe, AZ, USA and [2]School of Life Sciences, Arizona State University, Tempe, AZ, USA

Telomerase synthesizes telomeric DNA repeats onto chromosome termini from an intrinsic RNA template. The processive synthesis of DNA repeats relies on a unique, yet poorly understood, mechanism whereby the telomerase RNA template translocates and realigns with the DNA primer after synthesizing each repeat. Here, we provide evidence that binding of the realigned RNA/DNA hybrid by the active site is an essential step for template translocation. Employing a template-free human telomerase system, we demonstrate that the telomerase active site directly binds to RNA/DNA hybrid substrates for DNA polymerization. In telomerase processivity mutants, the template-translocation efficiency correlates with the affinity for the RNA/DNA hybrid substrate. Furthermore, the active site is unoccupied during template translocation as a 5 bp extrinsic RNA/DNA hybrid effectively reduces the processivity of the template-containing telomerase. This suggests that strand separation and template realignment occur outside the active site, preceding the binding of realigned hybrid to the active site. Our results provide new insights into the ancient RNA/DNA hybrid binding ability of telomerase and its role in template translocation.
The EMBO Journal (2012) **31,** 150–161. doi:10.1038/emboj.2011.363; Published online 11 October 2011
Subject Categories: genome stability & dynamics
Keywords: processivity; reverse transcriptase; telomere; template translocation

Introduction

Telomerase is a unique reverse transcriptase (RT) essential for *de novo* synthesis of telomeric DNA repeats onto chromosomal termini to counter progressive telomere shortening resulting from incomplete end replication (Zakian, 2009). The renewal capacity of highly proliferative cells, such as germline and stem cells, relies on telomere length maintenance by telomerase to offset cellular and organismal aging. A number of inherited human diseases, including dyskeratosis congenita, aplastic anaemia and idiopathic pulmonary fibrosis, are linked to telomerase gene mutations which result in telomere-mediated stem cell defects (Armanios, 2009). While undetectable in human somatic cells, telomerase is upregulated in most cancer cells and viewed as a promising therapeutic drug target (Shay and Keith, 2008). Thus, understanding the mechanism of telomerase is essential for developing therapies for cancer and telomere-mediated diseases as well as discerning cellular aging.

Telomerase functions as a ribonucleoprotein (RNP) enzyme, requiring two essential core components, the integral telomerase RNA (TR) and the telomerase reverse transcriptase (TERT) protein (Collins, 2008). The TERT protein contains the catalytic site for DNA polymerization and the TR provides a short template specifying the synthesized DNA sequence. The synthesis of a telomeric repeat requires the 3′-end of the DNA primer to base pair with the RNA template to form an RNA/DNA hybrid positioned within the active site. DNA polymerization then proceeds by reverse transcribing the RNA template to synthesize one telomeric repeat (GGTTAG in vertebrates) onto the 3′-end of the DNA primer. Outside the catalytic site, telomerase contains elements within both the TERT and TR necessary for RNP biogenesis and activity regulation (Autexier and Lue, 2006; Wyatt *et al*, 2010).

Within most species, the TERT protein is composed of four structural domains: the telomerase-essential N-terminal (TEN) domain, the telomerase RNA binding domain (TRBD), the RT domain and the C-terminal extension (CTE) domain. The central RT domain contains seven motifs (1, 2, A, B, C, D and E) that constitute the catalytic site and are evolutionarily conserved among all known RTs (Nakamura *et al*, 1997). The remaining three domains contain binding sites for single-stranded telomeric DNA and TR (Bryan *et al*, 2000; Peng *et al*, 2001; Moriarty *et al*, 2002; Huard *et al*, 2003; Jacobs *et al*, 2006). A recent crystal structure of the *Tribolium castaneum* TERT protein reveals that the TRBD, RT and CTE domains fold into a ring structure with a central cavity bound to an RNA/DNA hybrid (Gillis *et al*, 2008; Mitchell *et al*, 2010; Wyatt *et al*, 2010).

While the TERT protein is well conserved across eukaryotes, the TR component is divergent in size, sequence and secondary structure among distinct evolutionary lineages. The vertebrate TR folds into three structural domains: the template-pseudoknot, the CR4/5 and the H/ACA domains (Chen *et al*, 2000). The 3′ H/ACA domain is essential *in vivo* for biogenesis, while dispensable *in vitro* for telomerase activity (Collins, 2008). In contrast, the template-pseudoknot and CR4/5 domains are necessary for reconstituting telomerase activity *in vitro* and independently bind to the TERT protein (Tesmer *et al*, 1999; Mitchell and Collins, 2000). The template-pseudoknot domain positions the template proximal to the active site and contains a conserved pseudoknot structure with a triple helix crucial for telomerase function

*Corresponding author. Department of Chemistry and Biochemistry, Arizona State University, PO Box 871604, Tempe, AZ 85287, USA. Tel.: +1 480 965 3650; Fax: +1 480 965 2747;
E-mail: jlchen@asu.edu
[3]These authors contributed equally to this work
[4]Present address: Department of Molecular Biophysics and Biochemistry, Yale University, New Haven, CT 06520, USA

Received: 12 April 2011; accepted: 13 September 2011; published online: 11 October 2011

(Theimer *et al*, 2005; Qiao and Cech, 2008). The CR4/5 domain contains a conserved three-way helical junction that is also essential for telomerase activity (Chen *et al*, 2002).

A unique biochemical attribute of vertebrate and ciliate telomerase is repeat-addition processivity, whereby hundreds of DNA repeats can be synthesized onto a given DNA primer without complete dissociation from the enzyme (Lue, 2004). Telomerase processivity relies on a 'template translocation' mechanism to regenerate the RNA template after each repeat synthesized. Template translocation is defined as the separation of the RNA template from the DNA product, translocation and realignment with the DNA strand to regenerate the 5′-region of the RNA template for additional repeat synthesis. The template-translocation efficiency determines the repeat-addition processivity. In contrast, the template translocation rate limits the repeat-addition rate as indicated by the strong pause following each repeat synthesis, which produces the characteristic 6-base ladder banding pattern of telomerase extension products (Morin, 1989; Greider, 1991).

Many factors affecting processivity have been identified within the TERT, TR and accessory proteins. Within the human TERT (hTERT) protein, mutations in several conserved domains and motifs, such as TEN, motif 3, IFD (Insertion in Fingers Domain) and CTE, affect telomerase repeat-addition processivity (Xie *et al*, 2010). TEN functions as an anchor site which binds upstream single-stranded telomeric DNA, while motif 3, IFD and CTE are proposed to form a molecular clamp facilitating the formation and/or binding of the RNA/DNA hybrid during template translocation (Xie *et al*, 2010). In the TR, the template length determines repeat-addition processivity by affecting the template realignment efficiency (Chen and Greider, 2003). Accessory proteins such as the POT1–TPP1 complex in human and the Teb1–TASC complex in *Tetrahymena* dramatically increase repeat-addition processivity by concurrently binding the telomerase enzyme and the DNA products to delay complete dissociation (Wang *et al*, 2007; Latrick and Cech, 2010; Min and Collins, 2010; Zaug *et al*, 2010). Nonetheless, the detailed mechanism of telomerase template translocation remains enigmatic.

In this study, we provide data supporting the binding of the realigned RNA/DNA hybrid to the TERT active site as the final step in template translocation, which determines repeat-addition processivity. Our template-free human telomerase system demonstrates that the active site of telomerase binds directly to the RNA/DNA hybrid to catalyse RNA-dependent DNA synthesis. Furthermore, the affinity of telomerase processivity mutants for RNA/DNA hybrid substrates correlates with template-translocation efficiency. Lastly, we demonstrate that the active site of telomerase is accessible during template translocation, suggesting the realignment of the RNA template and the DNA primer occurs outside the active site. These results together provide important insights into the molecular mechanism of telomerase action.

Results

Template-free telomerase utilizes RNA/DNA hybrid as substrate

The mechanism for the TERT active site binding telomeric DNA and template RNA during a processive reaction is currently poorly understood. After each repeat synthesized, an uncharacterized mechanism regenerates the template by separating and translocating the RNA template from the extended DNA product and realigning the RNA with the DNA. Under standard conditions, telomerase utilizes single-stranded telomeric DNA as substrate, while conventional RTs utilize RNA/DNA hybrids as substrates. The conservation of essential motifs in the catalytic domain of both TERT and conventional RTs prompted us to examine the TERT active site for utilizing RNA/DNA hybrid substrates. Therefore, we designed and reconstituted a template-free human telomerase, in which the human TR (hTR) harbours a 5′-truncation (Δ1–63 nt), removing the template sequence. A similar template-free system was previously reported using *Tetrahymena* telomerase devoid of the template from the integral TR (Miller and Collins, 2002).

The template-free human telomerase was reconstituted *in vitro* in rabbit reticulocyte lysates (RRLs) using *in vitro* synthesized hTERT protein and two human TR fragments: the truncated pseudoknot PK-2 (hTR64-184) and CR4/5 (hTR239-328) (Figure 1A). As a control, a template-containing telomerase was also reconstituted using the longer pseudoknot PK-1 (hTR32-195) and CR4/5 (hTR239-328). As expected, the template-free telomerase did not extend a single-stranded telomeric DNA primer, while the template-containing telomerase added telomeric repeats processively (Supplementary Figure S1).

The reconstituted telomerases were assayed for activity with an RNA/DNA hybrid substrate composed of a 7 bp hetero-duplex with a 2-nt 5′ RNA overhang as template (Figure 1B). Remarkably, the template-free human telomerase recognized the RNA/DNA hybrid as substrate and added an α-^{32}P deoxyguanosine to the 3′-hydroxyl of the DNA primer to generate an 8-nt product (Figure 1B, lane 9). In the presence of dGTP and dTTP, both residues from the RNA overhang served as template to generate a 9-nt DNA product (Figure 1B, lane 10). Furthermore, an array of template sequences and lengths was tested to confirm that the number and identity of nucleotides synthesized onto the DNA primer were specified by the RNA template (Supplementary Figure S2). Thus, the template-free telomerase extended the DNA primer within the RNA/DNA hybrid in a template-dependent manner. In addition, the template-free telomerase catalysed the extension of only the RNA/DNA hybrid substrate. Single-stranded DNA or RNA oligo alone failed to produce similar activity (Figure 1B, lanes 11 and 12). Moreover, at temperatures above the melting temperature of 40.7°C for the duplex substrate, the template-free telomerase exhibited no activity (Supplementary Figure S3A and B). In contrast, the template-containing telomerase was catalytically active with the single-stranded DNA substrate at temperatures exceeding 50°C (Supplementary Figure S3C). This further supports that the template-free telomerase reacts specifically with the substrate as a hybrid. Nonetheless, the template-free telomerase exhibited a near-background level of terminal transferase activity in the presence of 20 μM DNA primer (Figure 1B, compare lanes 1 and 12). This is consistent with the previous report of the TERT protein acting as an RNA-independent terminal transferase under specific conditions (Lue *et al*, 2005).

While recognizing the RNA/DNA hybrid substrate like a conventional RT, the template-free human telomerase functioned as an RNP enzyme, requiring both the pseudoknot and CR4/5 RNA fragments for full activity (Figure 1B, compare

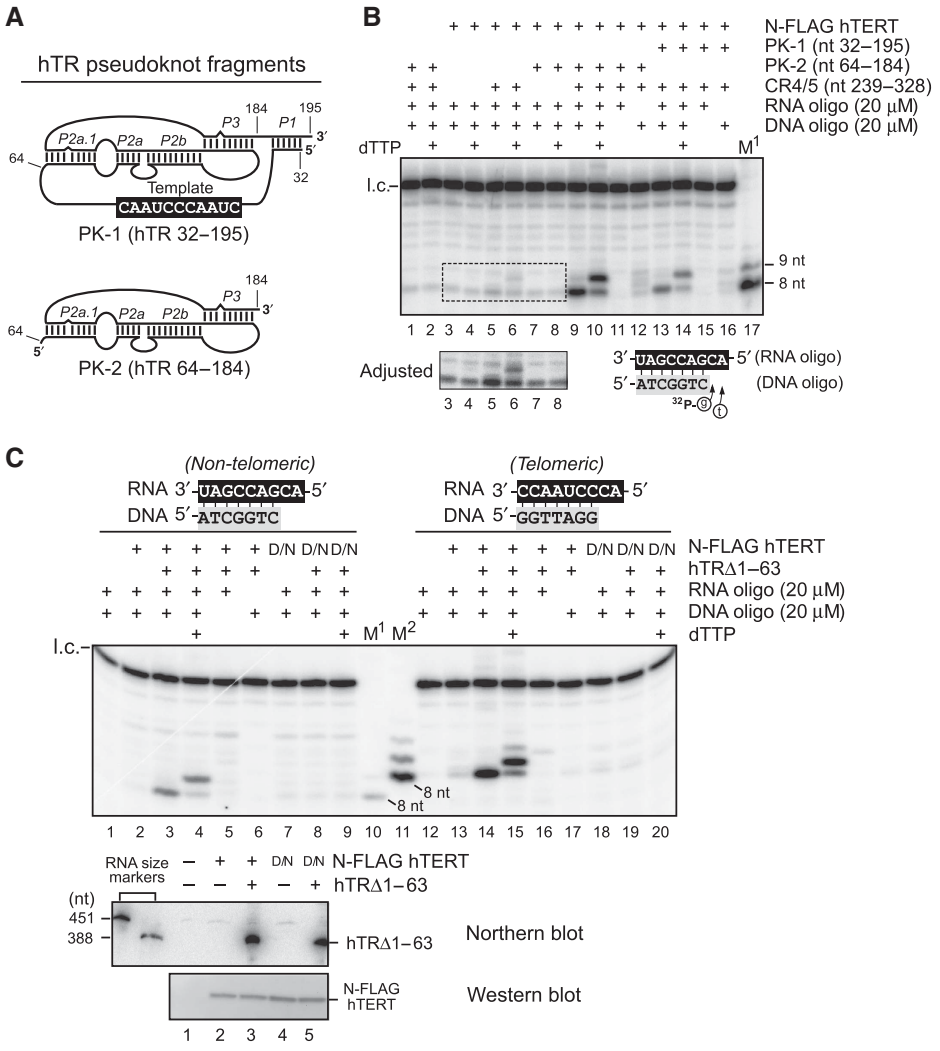

Figure 1 Template-free human telomerase extends RNA/DNA hybrid substrates. (**A**) Secondary structures of hTR pseudoknot fragments used for telomerase *in vitro* reconstitution. The RNA fragment PK-1 consists of hTR residues 32–195 which includes the template sequence. The RNA fragment PK-2 consists of hTR residues 64–184 which lacks both the template sequence and helix P1. (**B**) *In vitro* reconstituted template-free human telomerase extends an RNA/DNA hybrid substrate. Telomerase was reconstituted in RRL from the recombinant N-FLAG-hTERT protein, hTR pseudoknot (PK-1 or PK-2) and CR4/5 RNA (hTR 239–328) as indicated. Reconstituted telomerase was assayed for nucleotide-addition activity with 20 μM of RNA/DNA hybrid (7 bp duplex and 2 nt RNA 5′-overhang), or single-stranded RNA (5′-ACGACCGAU-3′) and DNA (5′-ATCGGTC-3′) oligonucleotides. The unpaired overhang (5′-AC) at the 5′-end of the RNA strand in the substrate served as the template for addition of α-^{32}P-dG and dT residues to the 3′-end of the DNA strand. The presence or absence of dTTP distinguished template-dependent nucleotide addition from terminal transferase activity. (*Adjusted*) A longer exposure of lanes 3–8 from the same gel. A DNA size marker (M^1) was generated by labelling the 3′-end of the DNA oligonucleotide (5′-ATCGGTC-3′) with α-^{32}P-dG using terminal deoxynucleotidyl transferase. A loading control (l.c.) was included in each reaction to ensure equal sample recovery. (**C**) Template-free human telomerase reconstituted in 293FT cells extends both non-telomeric and telomeric RNA/DNA hybrid substrates. 293FT cells were transiently transfected with either N-FLAG-hTERT or N-FLAG hTERT-D868N (D/N) genes in combination with the truncated hTR Δ1–63 gene to reconstitute template-free telomerase as labelled above the gel. Template-free telomerase activity assay was performed using immuno-purified FLAG-tagged telomerase complexes with either the non-telomeric (DNA: 5′-ATCGGTC-3′) or telomeric (DNA: 5′-GGTTAGG-3′) hybrid substrates. The DNA size marker (M^2) was generated by labelling the DNA oligonucleotide (5′-GGTTAGG-3′) with α-^{32}P-dG residues using terminal deoxynucleotidyl transferase. Northern blot was performed to detect the presence of hTRΔ1–63 in the immuno-purified telomerase complex. One nanogram of T7 transcribed hTR (451 nt) and hTRΔ1–63 (388 nt) were included as size markers. Western blot was performed to detect the N-FLAG-hTERT and N-FLAG-hTERT-D868N (D/N) recombinant proteins in the immuno-purified telomerase complex.

lanes 3 and 9). In the native template-containing telomerase, the pseudoknot domain is essential for positioning the template within the TERT active site. In the case of template-free telomerase, a low level of activity was detected from the enzyme lacking the PK-2 RNA, suggesting the pseudoknot domain is not absolutely necessary for telomerase catalysis (Figure 1B, lanes 5 and 6). One major function of the pseudoknot domain is to position the template to the active site. Within a template-free system, the active site binds directly to the RNA/DNA hybrid substrate, eliminating the need for the pseudoknot. This is further supported by the recent report that deletion of the TEN domain, which binds the pseudoknot domain, still allows synthesis of a single DNA repeat (Robart and Collins, 2011).

The template-containing telomerase reconstituted from the PK-1 (hTR32-195) RNA fragment also reacted with the RNA/

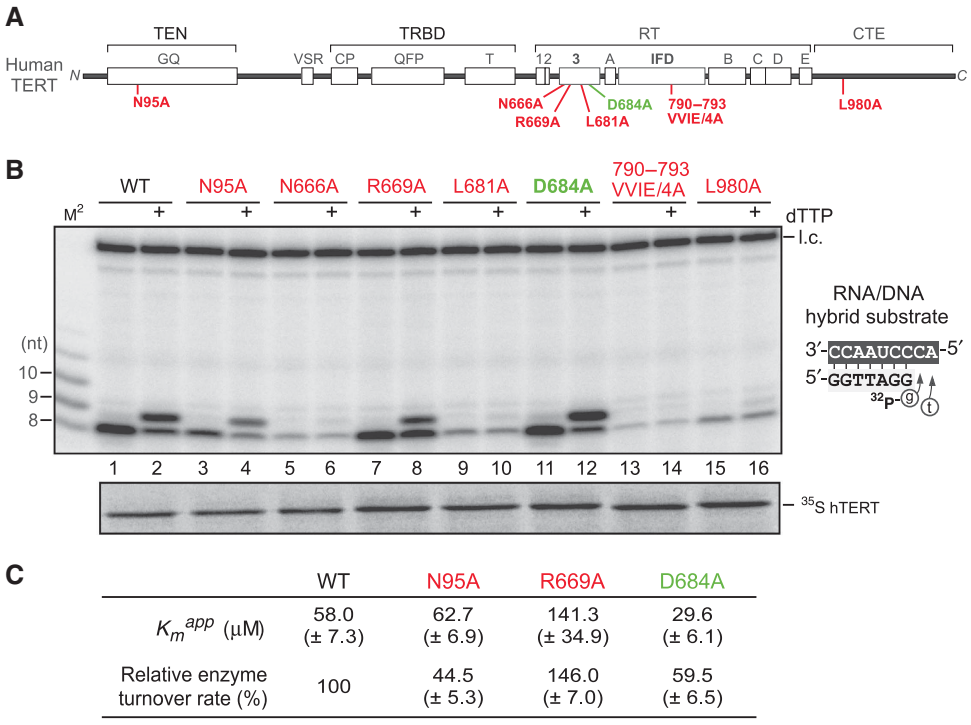

C

	WT	N95A	R669A	D684A
K_m^{app} (μM)	58.0 (± 7.3)	62.7 (± 6.9)	141.3 (± 34.9)	29.6 (± 6.1)
Relative enzyme turnover rate (%)	100	44.5 (± 5.3)	146.0 (± 7.0)	59.5 (± 6.5)

Figure 2 Effects of hTERT mutations on K_m and enzyme turnover rate to the RNA/DNA duplex substrate. (**A**) The positions of hTERT mutations that increase (green) or decrease (red) repeat-addition processivity are indicated on the schematic of domain/motif organization of hTERT protein. (**B**) The activity of template-free telomerase utilizing RNA/DNA hybrid substrate is affected by hTERT processivity mutations. Telomerase mutants were reconstituted *in vitro* from recombinant N-FLAG hTERT protein, hTR PK-2 and CR4/5 RNA fragments. Mutant enzymes were assayed in the presence or absence of dTTP with the telomeric RNA/DNA hybrid substrate (RNA-5′-ACCCUAACC-3′/DNA-5′-GGTTAGG-3′). The hTERT proteins labelled with ^{35}S-methionine were analysed by SDS–PAGE to quantify the levels of TERT. The DNA size marker (M^2) was prepared as described in Figure 1C. (**C**) Apparent K_m values and turnover rates of template-free processivity mutants (N95A, R669A and D684A) with the RNA/DNA hybrid substrate. Three independent experiments were performed to give rise to a mean value ± standard deviation for the K_m^{App} values.

DNA hybrid substrate generating weak activity (Figure 1B, lanes 13 and 14). This activity was independent of the intrinsic RNA template, since the non-telomeric DNA primer was non-complementary and unable to base pair with the intrinsic RNA (Figure 1B, compare lanes 13 and 16). This suggests the active site in the template-containing telomerase was accessible to bind the RNA/DNA hybrid.

In addition to the *in vitro* reconstituted enzyme, we assayed the *in vivo* reconstituted template-free telomerase for activity with RNA/DNA hybrid substrates. We reconstituted the template-free telomerase by ectopic overexpression of N-terminal FLAG-tagged hTERT protein and 5′-truncated (Δ1–63) hTR in 293FT cells. Ectopic overexpression was verified by western and northern blotting (Figure 1C, lower panel, compare lanes 1 and 3). The *in vivo* reconstituted template-free telomerase extended DNA primers within both telomeric and non-telomeric RNA/DNA hybrid substrates, while the telomeric substrates produced a higher level of activity (Figure 1C, lanes 3, 4, 14 and 15). As a control, a telomerase reconstituted from a catalytically inactive TERT mutant (D868N) failed to show any RT activity (Figure 1C, lanes 7–9 and 18–20).

RNA/DNA hybrid substrate binding affinity correlates with repeat-addition processivity and template-translocation efficiency

At the end of a template translocation cycle, the realigned RNA/DNA hybrid must reposition within the active site for nucleotide addition. We propose that the binding affinity of the RNA/DNA hybrid to the active site directly affects the template-translocation efficiency and determines repeat-addition processivity. Thus, a lower affinity for the hybrid substrate is expected to result in lower template-translocation efficiency. This hypothesis was tested by generating template-free versions of telomerase mutants known to have altered repeat-addition processivity and measuring their activity with the RNA/DNA hybrid substrate. These TERT mutations examined are located in three distinct structural domains: the TEN domain (N95A), motif 3 in the RT domain (N666A, R669A, L681A and D684A) and IFD (790-793VVIE/4A), and the CTE domain (L980A) (Figure 2A). All these mutations decreased repeat-addition processivity, except D684A which increased processivity (Supplementary Figure S4; Xie *et al*, 2010). The low-processivity TERT mutants (N666A, L681A, 790-793VVIE/4A and L980A) failed to extend the RNA/DNA hybrid substrate (Figure 2B, lanes 5, 9, 13 and 15), while the increased processivity mutant D684A retained wild-type level activity (Figure 2B, lanes 11 and 12). The TEN domain N95A mutation did not significantly alter the activity with the hybrid substrate (Figure 2B, lanes 3 and 4). This was expected, as the TEN domain mutation N95A has been shown to affect processivity by reducing single-stranded DNA binding and increasing the rate of complete product-dissociation from the enzyme (Wyatt *et al*, 2007). However, the strong activity from the low-processivity motif-3 R669A mutant was not predicted (Figure 2B, lanes 7 and 8).

The effects of these mutations on substrate affinity were examined by measuring the Michaelis constant (K_m) for the RNA/DNA hybrid substrate in the template-free system. The decreased processivity mutant R669A had a K_m^{app} value of 141 μM, which was considerably higher than the 58 μM for the wild-type enzyme. In contrast, the high-processivity D684A mutant exhibited a decreased K_m^{app} of 29.6 μM (Figure 2C). Thus, the K_m inversely correlates with processivity. However, the K_m also includes the rate at which the enzyme-bound substrate is converted to free product. Under the general assumption that this rate is limiting, K_m approximates the substrate binding affinity (Northrop, 1998). These results show a strong correlation between repeat-addition processivity and K_m for the duplex substrate.

To further investigate the unexpected higher overall activity of the R669A mutant, we measured the relative enzyme turnover rates of the mutants with a time-course assay. The R669A mutant had a 50% higher rate than the wild-type enzyme, and the D684A mutant had a decreased enzyme turnover rate (Figure 2C). These data suggest that the higher overall activity of the R669A mutant resulted from faster enzyme turnover.

Repeat-addition processivity is determined by the efficiency of template translocation. We thus investigated the translocation efficiency of mutants with different duplex binding affinities. The efficiency was measured by a single-translocation assay, whereby only a single template translocation event can occur and the reaction pauses from the absence of dTTP during nucleotide addition of the second repeat (Latrick and Cech, 2010). Telomerase enzymes containing the TERT mutations were reconstituted *in vitro* and incubated with the 20 nt telomeric DNA primer 5′-TT(AGGGTT)$_3$-3′ prior to initiating the primer extension reaction (Figure 3A). Additionally, a 10-fold excess of an unextendable DNA competitor, 5′-(TTAGGG)$_3$-3′-amine, was added to the reaction to minimize enzyme turnover. The expected 22-nucleotide (+2 nt) product prior to a template translocation was seen at the 2-min time point (Figure 3B, lane 1). After translocation, two more residues were added to generate the 24-nucleotide (+4 nt) product (Figure 3B, lanes 2–4). The faint 23-nucleotide (+3 nt) product was unrelated to template translocation, but likely produced from telomerase terminal transferase activity. In support of this, the hTR55G mutation that reduces template-translocation efficiency did not alter the intensity of the +3-nt band (Supplementary Figure S5). We calculated the translocation efficiency of each TERT mutant by measuring the ratio of post-translocation products (+4 nt) over the total products (+2 and +4 nt) at the final time point. Prolonged reaction time courses (60, 90 and 120 min) ensured the maximum translocation efficiency was reached.

The mutants with low RNA/DNA hybrid substrate affinity had low translocation efficiency (Figure 3B and C). The only exception was the N95A mutant, which was defective outside the active site and retained normal substrate affinity to the RNA/DNA hybrid. The increased processivity mutant D684A had high substrate binding affinity to the RNA/DNA hybrid and high translocation efficiency. The K_m to the duplex substrate strongly correlated with the repeat-addition processivity and template translocation efficiency of the mutants (Figure 3D), suggesting the binding of RNA/DNA hybrid to the active site is a key determinant of template-translocation efficiency.

Duplex length affects enzyme turnover and nucleotide-addition processivity, while K_m is unchanged

In human telomerase, successful template translocation results in a 5 bp realigned RNA/DNA hybrid positioned inside the active site for the next repeat synthesis. The additional base pairs synthesized onto the hybrid during nucleotide addition could potentially (1) extend the hybrid to 10 bp or (2) induce base-pair dissociation at the other end to maintain a constant hybrid length. To distinguish between these two possibilities, we assayed *in vitro* reconstituted template-free telomerase with RNA/DNA hybrid substrates from 5 to 10 bp in length. The low melting temperatures (17–19°C) of the short 5 and 6 bp hybrids required assaying at 4°C to prevent denaturing the RNA/DNA hybrid substrate (Figure 4A, right panel; Supplementary Figure S6). Interestingly, the shorter 5 and 6 bp hybrid substrates resulted in significantly higher overall activity compared with the longer hybrids (Figure 4A, lanes 2–5). The higher activity could result from either higher substrate affinity or higher enzyme turnover. We measured both the K_m and enzyme turnover rate for the 5, 7 and 9 bp hybrid substrates. The turnover rate of the 5-bp substrate was 25-fold higher than the longer 9 bp substrate, while maintaining a similar K_m^{app} between 20 and 30 μM (Figure 4A, right panel). The higher enzyme turnover rate suggests that the shorter 5 bp duplex is a more efficient substrate for the template-free telomerase.

The duplex length also affected nucleotide-addition processivity. A 5-bp hybrid substrate can only be extended by a single nucleotide regardless of the template length or sequence (Figure 4A, lanes 2 and 3; Supplementary Figure S7, lanes 4–6). In contrast, a 6 bp hybrid substrate can be extended 2 nt (Figure 4A, lanes 3 and 4). We suspect the longer duplex might transiently generate a single-stranded DNA or RNA overhang at the duplex end distal the active site. The potential effects of overhangs in the RNA/DNA hybrid substrates on nucleotide-addition processivity were assayed with substrates containing a 5 bp hybrid and either a 3′ RNA or 5′ DNA overhang (Figure 4C). The duplex substrates with 5′ DNA overhangs were extended by the addition of two nucleotides in the presence of dTTP, while the substrate with the 3′ RNA overhangs failed to extend beyond a single nucleotide (Figure 4B, lanes 4, 6, 8 and 10). This suggests that a putative TERT active site proximal anchor site binds the 5′ DNA overhang on the 5-bp RNA/DNA hybrid to facilitate nucleotide-addition processivity. In addition, the K_m^{app} of the 5-bp substrates with the 2-nt 5′ DNA overhang is ~5 μM, substantially lower than the 15 μM for the substrate with a single nucleotide DNA overhang (Figure 4C). Thus, the presence of a DNA residue at the −7 position is important for binding affinity of the 5-bp RNA/DNA hybrid to the active site (Figure 4D).

Active site of telomerase is accessible during template translocation

Since the active site binding the RNA/DNA hybrid is crucial for template-translocation efficiency, we expect the realignment of the RNA template and DNA primer to occur outside the active site, leaving the active site temporarily unoccupied. The accessibility of the active site during processive repeat

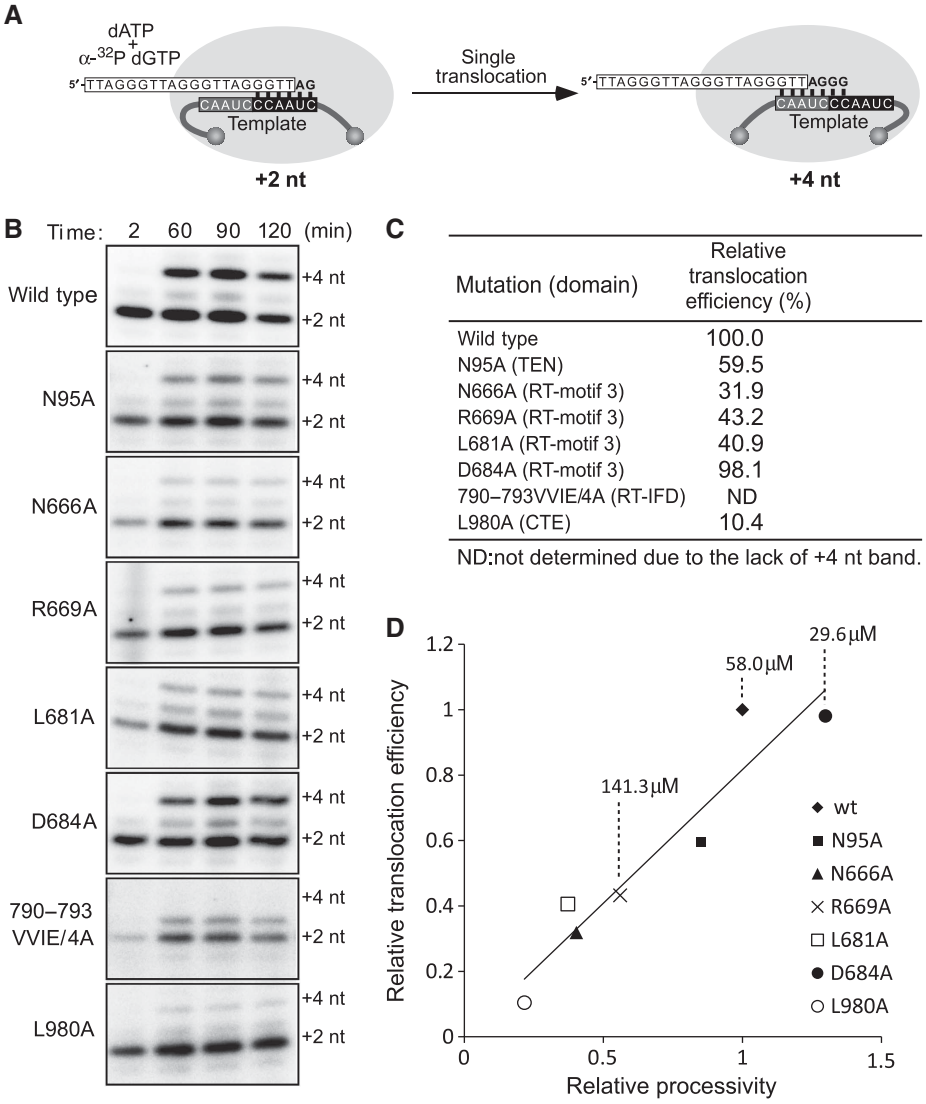

Figure 3 Template-translocation efficiency of telomerase processivity mutants. (**A**) Schematic of the single-translocation assay. In the presence of dATP and α-^{32}P-dGTP, telomerase adds two residues (dA and α-^{32}P-dG) to the DNA primer, resulting in a +2 nt product. After template translocation, telomerase adds two additional dG residues, generating a +4-nt product. The reaction pauses from the lack of dTTP. (**B**) Single-translocation time-course assays of telomerase processivity mutants. Immuno-purified, *in vitro* reconstituted telomerase mutants containing TERT processivity mutations (N95A, N666A, R669A, L681A, D684A, 790-793VVIE/4A and L980A) were analysed to determine the translocation efficiencies. Enzymes were incubated with the DNA primer 5′-TT(AGGGTT)$_3$-3′ prior to the time-course assay (2, 60, 90 and 120 min). The major bands for pre-translocation (+2 nt) and post-translocation (+4 nt) products are indicated. (**C**) Translocation efficiency of telomerase processivity mutants. The translocation efficiencies of the wild-type and mutant telomerases were determined by dividing the intensity of post-translocation bands (+4 nt) by the intensity of all bands (+2 and +4 nt) from the reaction at the 120-min time point shown in Figure 3B. (**D**) Correlation between the K_m for the duplex substrate, relative translocation efficiency and repeat-addition processivity of the hTERT mutants. The relative translocation efficiencies were plotted against the relative repeat-addition processivity. The K_m^{app} values of the wild-type, R669A and D684A mutants for duplex substrate are labelled.

addition was assayed by a 'pulse and chase/challenge', in which a short RNA/DNA hybrid was added in the chase reaction to compete against the intrinsic, realigned RNA/DNA hybrid for the active site. A telomeric 18-mer DNA primer (TTAGGG)$_3$ was first extended by *in vivo* reconstituted, template-containing telomerase in a 15-min 'pulse' reaction containing α-^{32}P-dGTP, dATP and dTTP. The pulsed reaction was then chased and challenged with 600-fold non-radioactive dGTP and 200 μM of excess 5 or 7 bp RNA/DNA hybrid. The pulse and chase/challenge reactions were performed at 4°C to prevent denaturation of the short duplexes.

Our results indicate the 5 bp RNA/DNA hybrid competes effectively for the active site, reducing repeat-addition processivity of the enzyme during the chase/challenge reaction (Figure 5, compare lanes 2 and 4). In contrast, the longer 7 bp duplex failed to inhibit repeat-addition processivity (Figure 5, compare lanes 2 and 8), suggesting the active site has a limited accessibility for only the short duplex during template translocation. In the control reactions, the RNA oligonucleotide alone also slightly decreased repeat-addition processivity (Figure 5, lanes 5 and 9), possibly by interacting with the telomeric DNA undergoing template translocation. Non-specific labelling of the competing duplexes (Figure 5, lanes 3–4

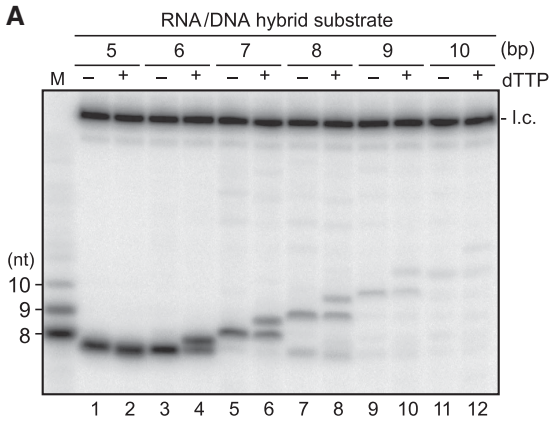

(bp)	Sequence	T_m (°C)	K_m^{app} (μM)	Relative turnover (%)
5	3′-AUCCCCA-5′ 5′-TAGGG	17.0	29.1±2.1	100
6	3′-AAUCCCCA-5′ 5′-TTAGGG	19.4	ND	ND
7	3′-CAAUCCCCA-5′ 5′-GTTAGGG	30.3	38.2±12.9	22.5±2.6
8	3′-CCAAUCCCCA-5′ 5′-GGTTAGGG	40.6	ND	ND
9	3′-CCCAAUCCCCA-5′ 5′-GGGTTAGGG	49.6	22.4±3.4	4.2±2.9
10	3′-UCCCAAUCCCCA-5′ 5′-AGGGTTAGGG	57.3	ND	ND

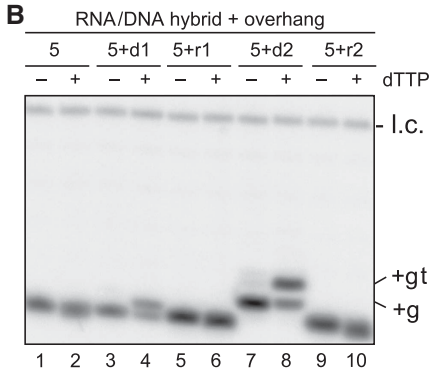

	Sequence	K_m^{app} (μM)
5 bp	3′-AUCCCCA-5′ 5′-TAGGG	17.1 ± 2.2
5+d1	3′-AUCCCCA-5′ 5′-TTAGGG	18.0 ± 0.6
5+r1	3′-AAUCCCCA-5′ 5′-TAGGG	15.5 ± 0.8
5+d2	3′-AUCCCCA-5′ 5′-GTTAGGG	5.2 ± 0.7
5+r2	3′-CAAUCCCCA-5′ 5′-TAGGG	15.0 ± 0.8

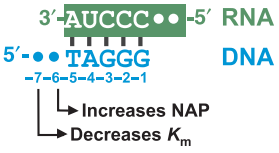

Figure 4 Effect of the RNA/DNA hybrid length on K_m, enzyme turnover rate and nucleotide-addition processivity. (**A**) Effect of substrate-duplex length on activity of template-free telomerase. (*Left*) *In vitro* reconstituted template-free telomerase was assayed at 4°C with RNA/DNA hybrid substrates with duplex lengths ranging from 5 to 10 bp. Different product patterns in the presence or absence of dTTP demonstrate template-dependent DNA synthesis. (*Right*) Sequences, T_m, K_m and enzyme turnover rates of RNA/DNA hybrid substrates. The melting temperatures (T_m) of the duplexes were measured by UV melting curve analysis (see Materials and methods and Supplementary Figure S5). The values of K_m and relative turnover rates are given as the mean ± standard deviation derived from three independent experiments. DNA size marker (M) was generated by 3′-end α-^{32}P-dG labelling the 7-base DNA oligonucleotide (5′-GTTAGGG-3′) using terminal deoxynucleotidyl transferase. (**B**) Effects of overhangs of RNA/DNA hybrid substrates on nucleotide-addition processivity. The RNA/DNA hybrid substrates contain a 5 bp duplex and a 1–2 nt overhang at either the 5′ DNA (5 + d1 and 5 + d2) or the 3′ RNA (5 + r1 and 5 + r2) end. A ^{32}P end-labelled 15 nt DNA oligonucleotide was used as a loading control (l.c.). (**C**) K_m of RNA/DNA hybrid substrates with and without overhangs. Sequences and structures of the RNA/DNA hybrid substrates are shown. (**D**) Diagram of RNA/DNA hybrid substrate indicating nucleotides important for nucleotide-addition processivity (NAP) and K_m.

and 7–8) or the RNA oligonucleotides (Figure 5, lanes 5 and 9) was also observed. These activities were not derived from telomerase, as they were also observed with catalytically inactive telomerases (Supplementary Figure S8). Thus, the active site of telomerase during template translocation is at least transiently unoccupied and accessible to binding a 5 bp RNA/DNA hybrid.

Discussion

Telomerase has the unique ability to add multiple DNA repeats processively by iterative use of its short intrinsic RNA template. Repeat-addition processivity requires a special template-translocation mechanism involving strand separation of the RNA/DNA hybrid, physical movement of the RNA template relative to the DNA strand, reannealing of the RNA template to the DNA strand and finally repositioning of the hybrid within the TERT active site. In this study, by using our template-free human telomerase enzymes and RNA/DNA hybrid substrates, we demonstrate the active site of telomerase intrinsically binds the RNA/DNA hybrid (Figures 1 and 4). The correlation between the K_m of the RNA/DNA hybrid substrate and the repeat-addition processivity suggests binding of the realigned RNA/DNA hybrid to the active site is critical for template-translocation efficiency (Figures 2 and 3). Furthermore, our 'pulse and chase/challenge' assay of *in vivo* reconstituted, template-containing telomerase revealed the active site is unoccupied during template translocation (Figure 5), indicating the template RNA and primer DNA realign outside the active site. Collectively, our results provide important insights into the molecular mechanism of telomerase template translocation.

Length of RNA/DNA hybrid during nucleotide addition

In human telomerase, a 5 bp RNA/DNA hybrid is formed upon completion of template translocation, and ready for nucleotide addition (Figure 6A). Chemical modification probing of the RNA template in yeast telomerase indicates the number of base pairs in the RNA/DNA hybrid remains constant during successive nucleotide addition (Forstemann and Lingner, 2005). Thus, the formation of each new base pair from nucleotide addition is accompanied by disruption

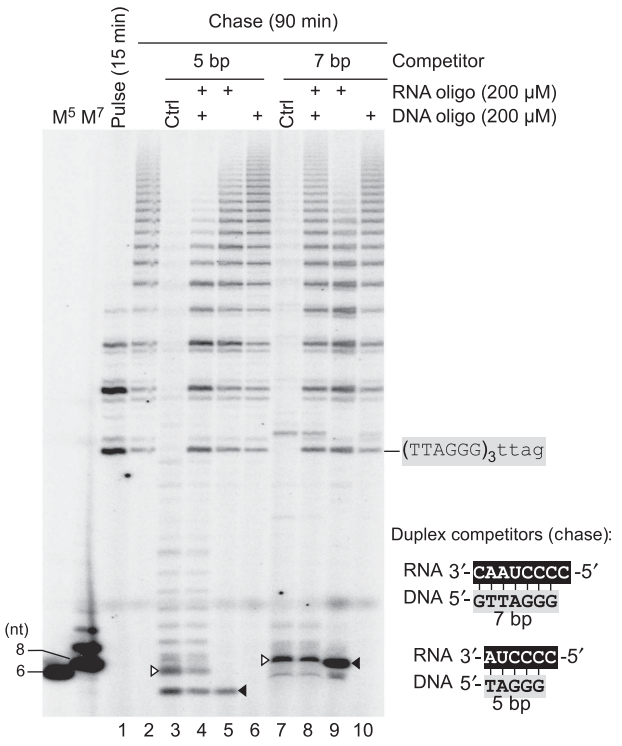

Figure 5 A 5-bp RNA/DNA hybrid competitor inhibits repeat-addition processivity. Native template-containing telomerase reconstituted in 293FT cells was used in the pulse-chase/challenge assay. Two RNA/DNA duplexes (5 and 7 bp) were used as competitors to challenge the processive telomerase during the 90-min chase reaction at 4°C. The pulse reaction was carried out in the presence of α-^{32}P-dGTP for 15 min to radioactively label the telomeric DNA primer $(TTAGGG)_3$. The chase reaction was initiated by adding non-radioactive dGTP to 100 μM to eliminate products generated by recycling enzymes during the chase reaction. In addition, 200 μM of 5 or 7 bp RNA/DNA duplex competitors was added simultaneously in the chase reactions as indicated. Sequences and structures of the duplex competitors and telomeric single-stranded DNA primer are shown. A chase-only control (Ctrl) demonstrates the extended products of the telomeric DNA primer were only from the pulse reaction. Open triangle: non-specific products labelled from the RNA/DNA duplex (see Supplementary Figure S8). Filled triangle: non-specific products labelled from the RNA oligonucleotide (see Supplementary Figure S8). DNA size markers were generated by 3′-end labelling of the 5 and 7-base DNA oligonucleotide (M^5: TAGGG and M^7: GTTAGGG) using α-^{32}P-dGTP and terminal deoxynucleotidyl transferase.

of a previous base pair at the opposite end of the RNA/DNA hybrid. Within human telomerase, the conservation of this mechanism would result in the RNA/DNA hybrid remaining at 5 bp during nucleotide addition. From our data, shortening the RNA/DNA hybrid length to 5 bp significantly increases the enzyme turnover rate in the template-free telomerase system (Figure 4A). This suggests that the 5 bp duplex is a better substrate than the longer duplexes. Furthermore, the recent crystal structures of the *Tribolium* TERT show a central cavity that accommodates a short 5 bp duplex through physical protein–nucleic acid contacts (Mitchell *et al*, 2010).

Telomerase, like other conventional RTs, is capable of processive nucleotide addition onto a DNA primer, requiring physical movement of the RNA/DNA hybrid away from the active site following the addition of each nucleotide. A single unpaired DNA residue 5′ to the RNA/DNA hybrid is necessary and sufficient to facilitate duplex translocation with template-free telomerase and allow processive nucleotide addition (Figure 4B, lane 4). In contrast, an RNA overhang 3′ to the hybrid has no effect on duplex translocation (Figure 4B, lane 5). This suggests a protein–DNA interaction, whereby TERT binding to the unpaired residue on the DNA strand is required for duplex translocation. Previously, a DNA-binding anchor site on the TERT protein proximal to the active site has been proposed (Wyatt *et al*, 2007; Finger and Bryan, 2008). In addition to promoting nucleotide-addition processivity, the interaction between the proximal anchor site and the single-strand DNA could actively maintain a constant 5 bp RNA/DNA hybrid by breaking a single base pair in the duplex when a new base pair is formed. Such a mechanism would also explain how telomerase is capable of adding multiple repeats onto a short primer that, when base paired with the template, lacks any single-stranded overhang (Xie *et al*, 2010).

A working model of telomerase template translocation

Based on new insights from this study, we hereby propose a working model for the mechanism of telomerase template translocation (Figure 6). In our model, template translocation begins with duplex dissociation from the active site, followed by strand separation of the duplex, realignment of the template and primer, and finally binding of the realigned RNA/DNA hybrid by the active site. Below we detail the initial and final steps of this proposed mechanism.

The first step of template translocation. Template translocation requires RNA/DNA strand separation. It has, however, been unclear whether this occurs inside or outside the active site. In our model, duplex dissociation occurs outside the active site because it requires a relatively minor conformational change of the active site. Within the *Tribolium* TERT structure, only a minor difference in the diameter of the central cavity was observed when bound to an RNA/DNA hybrid (Mitchell *et al*, 2010). Strand separation within the active site would require substantial conformational changes in the TERT protein to unpair the duplex. Additionally, the hyperactive R669A mutant that exhibited increased repeat addition rate showed a higher enzyme turnover rate within our template-free system (Figure 2C). This suggests duplex dissociation is the rate-limiting step for template translocation. Furthermore, our 'pulse and chase/challenge' assay with the template-containing telomerase revealed the active site is transiently unoccupied during template translocation and capable of binding a 5 bp duplex (Figure 5, lane 4). Interestingly, the 7 bp duplex did not alter telomerase processivity (Figure 5, lane 8), suggesting the active site can only accommodate a shorter 5 bp duplex during template translocation.

Another attractive feature of having RNA/DNA strand separation occur outside the active site is that it does not require exogenous energy. Inside the active site, protein–nucleic acid interactions would presumably have to be disrupted to achieve strand separation. However, outside the active site, a 5–6 bp duplex would spontaneously dissociate very quickly. The off rate (k_{off}) of the 6 bp RNA/DNA hybrid (CUAACC/GGTTAG), approximated using the nearest neighbour thermodynamic parameters, is near 3 ms^{-1} at 37°C, which is equivalent to a half-life ($T_{1/2}$) of 0.2 ms (Sugimoto *et al*, 1995; Turner, 2000).

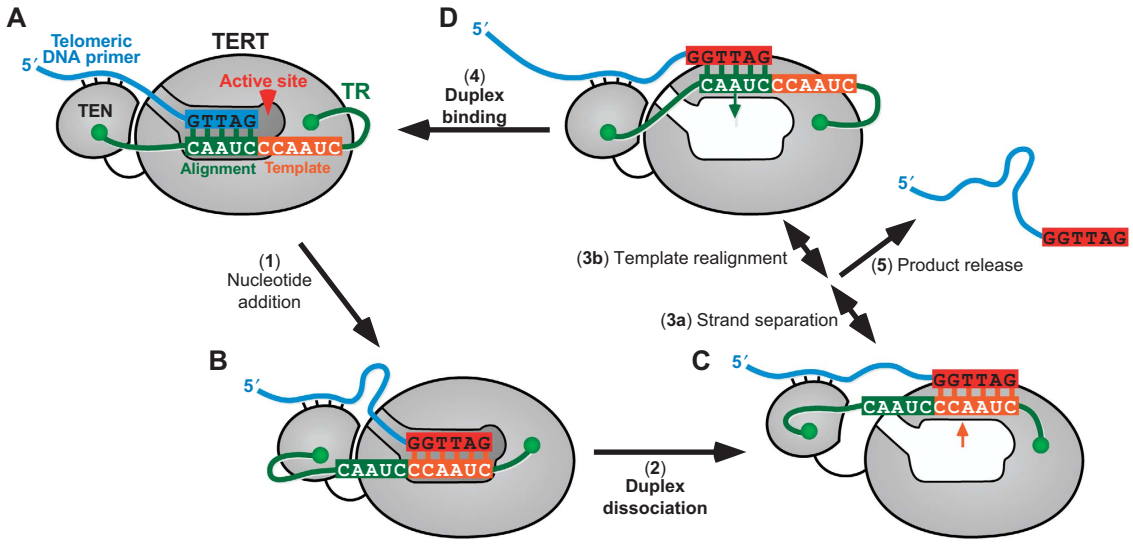

Figure 6 A working model for telomerase template translocation. (**A**) A schematic drawing of the human telomerase enzyme bound to the telomeric DNA substrate. Prior to repeat synthesis, the hTR alignment region (green) base pairs with the 3′-end of the telomeric primer DNA (blue) to form a 5 bp RNA/DNA hybrid within the active site. The RNA template is constrained by flanking sequences bound to the TERT protein, while the 5′ region of the telomeric DNA is bound to the TEN domain. The TERT protein catalyses polymerization of six deoxyribonucleotides to the 3′-end of the DNA primer by reverse transcribing the hTR template sequence (orange) (step 1). (**B**) After nucleotide addition, a new repeat (red) is generated, while the RNA/DNA hybrid length remains constant at the initial 5 bp. Upon reaching the end of the template, the RNA/DNA duplex dissociates from the active site (step 2). (**C**) Outside the active site, the RNA/DNA duplex undergoes strand separation (step 3a), and the DNA reanneals to either the alignment or the template regions. If the DNA reanneals to the template region, the result is non-productive, requiring further strand separation and a new attempt at reannealing. If the DNA reanneals to the alignment region (step 3b), the RNA template is regenerated. Both strand separation and realignment are presumably reversible, as indicated by the double-headed arrows. (**D**) The realigned RNA/DNA hybrid is then recaptured by binding to the active site (step 4) for further nucleotide addition. Unsuccessful reannealing of the DNA primer to the RNA template results in complete dissociation of the product from the enzyme (step 5).

Duplex binding to the active site is the final step in template translocation. Following the realignment of the RNA template and DNA primer, the resulting 5 bp hybrid is predicted to be relatively unstable with a low melting temperature (Figure 4A). Binding to the active site through protein–nucleic acid interactions would stabilize the hybrid and enhance template-translocation efficiency. In the template-free telomerase, there is a strong correlation between repeat-addition processivity and substrate binding affinity for the RNA/DNA hybrid. The hyper-processive D684A mutant has a low K_m^{app} value of 29.6 μM, while the hypo-processive R669A mutant has a high K_m^{app} value of 141.3 μM (Figure 2C; Supplementary Figure S4). This is further supported by the previous data that show a correlation between repeat-addition processivity and the K_m of motif 3 mutants for short 8 nt primers (Xie *et al*, 2010). In our model, these short primers will base pair with the template RNA outside the active site, independent of upstream DNA binding, and be positioned at the active site as an RNA/DNA hybrid. This explains why affinities to the short primer and the RNA/DNA hybrid correlate with telomerase repeat-addition processivity. However, the binding affinity of the 5 bp RNA/DNA hybrid to the template-free telomerase is relatively low, with a K_m^{app} around 30 μM (Figure 4A). This is not surprising since the native telomerase binds telomeric DNA primer primarily through the TEN domain and the RNA template is tethered to the integral TR.

The efficiency of template translocation is enhanced by promoting RNA/DNA hybrid binding to the active site (Figure 6D, step 4), or by delaying complete dissociation of the DNA product from the enzyme (Figure 6D, step 5). The TEN domain binds the 5′-region of the single-stranded telomeric DNA (Jacobs *et al*, 2006) and functions as an anchor site, preventing product release during translocation while not affecting duplex binding. Accessory proteins POT1 and TPP1 form a complex that reduces the dissociation rate of the DNA product from the enzyme (Latrick and Cech, 2010). As expected, the presence of the POT1–TPP1 complex did not affect the substrate binding affinity of the active site to the RNA/DNA hybrid within the template-free telomerase system (Supplementary Figure S9).

TERT and conventional RTs are evolutionarily related, descending from a common ancestor (Nakamura and Cech, 1998; Curcio and Belfort, 2007). While of RNA/DNA hybrids are the substrate of conventional RTs, the native substrate of telomerase is single-stranded telomeric DNA. However, the telomerase active site has retained the ability to bind RNA/DNA hybrids for efficient template translocation. In this study, we provide evidence that active site binding of RNA/DNA hybrid directly affects template-translocation efficiency, and thus processivity. Future elucidation of the rates of individual steps during template translocation will improve our understanding of the molecular mechanism of telomerase action.

Materials and methods

Oligonucleotides and RNA/DNA hybrid substrates

All RNA and DNA oligonucleotides were purchased from Integrated DNA Technologies (IDT). The sequences of oligonucleotides used in each experiment are shown in the text or figures. The RNA/

DNA duplexes were prepared by adding the RNA and complementary DNA oligos at a final concentration of 100 μM in 1 × annealing buffer (100 mM Tris–HCl pH 7.5, 500 mM NaCl and 50 mM EDTA). Duplex formation was facilitated by incubation at 70°C for 3 min, followed by slowly cooling to room temperature. Single-stranded RNA and DNA oligo controls were prepared the same way. The melting temperature (T_m) of the duplex was determined by measuring the OD_{260} of the duplex in solution with temperature decreasing from 70 to 0°C at −1°C/min using a Cary 300 UV-Vis spectrophotometer (Varian Tech.) with a multicell holder and a temperature controller. The OD_{260} of the duplex was measured under the activity assay condition with 20 μM DNA/RNA duplex in 1 × telomerase reaction buffer (50 mM Tris–HCl pH 8.3, 50 mM KCl, 2 mM DTT, 3 mM $MgCl_2$, 1 mM spermidine) and 0.2 × annealing buffer. The T_m values of the duplexes were determined by fitting data points to a sigmoidal curve (variable slope) using Prism (Graphpad Software Inc.).

Plasmid construction and mutagenesis

N-terminal FLAG-tagged hTERT protein was expressed *in vivo* from pcDNA-FLAG-hTERT, constructed by inserting the FLAG tag sequence into the pcDNA-hTERT vector (a kind gift from Dr Joachim Lingner). Catalytically inactive hTERT mutation D868N was introduced into pcDNA-FLAG-hTERT vector by site-directed mutagenesis using overlapping-extension PCR (Wu *et al*, 2005), generating pcDNA-FLAG-hTERT-D868N. The hTERT mutant plasmids for *in vitro* expression were constructed as previously described (Xie *et al*, 2010). The pBS-U1-hTRΔ1–63 for *in vivo* expression of the truncated, template-free hTRΔ1–63 was derived from pBS-U1-hTR (a gift from Dr Joachim Lingner) using overlapping PCR followed by subcloning.

Reconstitution of telomerase

Reconstitution of human telomerase *in vitro* was carried out in RRL as previously described (Xie *et al*, 2010). Briefly, hTERT was expressed from pN-FLAG-hTERT using the TnT® T7 Quick coupled transcription/translation kit (Promega) according to the manufacturer's instruction. The hTR fragments, PK-1 (nt 32–195), PK-2 (nt 64–184) and CR4/5 (nt 239–328), were transcribed *in vitro*, gel purified and added at a final concentration of 1 μM to assemble with hTERT in RRL. For quantification, hTERT was synthesized in the presence of ^{35}S-Methionine (>1000 Ci/mmol, 10.2 mCi/ml, Perkin-Elmer) and analysed by SDS–PAGE.

Reconstitution of human telomerase *in vivo* was carried out in 293FT cells using the overexpression system developed by Cristofari and Lingner (2006) with minor modifications. 293FT cells (Invitrogen) were grown in DMEM medium supplemented with 10% FBS, 1 × Penicillin-Streptomycin-Amphotericin mix (Lonza) and 5% CO_2 at 37°C. Prior to transfection, cells were seeded at $3–5 \times 10^5$ cells/well in a six-well plate and grown overnight. At 80–90% confluency, cells were transfected using 8 μl of Fugene HD transfection reagent (Roche) and 2 μg of plasmid DNA. The plasmid DNA mixture contained 0.4 μg of pcDNA-FLAG-hTERT and 1.6 μg of pBS-U1-hTR or pBS-U1-hTRΔ1–63, the ratio for maximum yield of active telomerase complex (Cristofari *et al*, 2007). After 48 h, transfected cells were harvested and homogenized in lysis buffer (10 mM Tris–HCl pH 7.5, 400 mM NaCl, 1 mM EGTA, 0.5% CHAPS, 1 mM $MgCl_2$, 10% glycerol, 5 mM β-mercaptoethanol, 1 × complete protease inhibitor cocktail (Roche)).

Immuno-purification of telomerase

Telomerase reconstituted *in vitro* and *in vivo* was immuno-purified by the N-terminal FLAG tag of the recombinant hTERT protein using monoclonal anti-FLAG antibody (M2) coated agarose beads (Sigma-Aldrich). Fifty microliters of reconstituted telomerase was mixed in a siliconized tube with 15 μl of pre-washed beads in TBS buffer (50 mM Tris–HCl pH 7.4 and 150 mM NaCl), and incubated at 4°C with gentle agitation for 2 h. The beads were then washed three times with 500 μl of TBS buffer and once with 1 × telomerase reaction buffer. The washed beads were either used directly for telomerase activity assay or resuspended in 1 × SDS–PAGE loading buffer (see below) for western blotting.

Western blotting

Immuno-purified telomerase complex was heated to 95°C for 5 min in 1 × SDS–PAGE loading buffer (0.125 M Tris–HCl pH 6.8, 2% SDS, 10% glycerol, 5% 2-mercaptoethanol and 0.0025% bromophenol blue), resolved on a 6% SDS–PAGE gel, and electrotransferred onto a PVDF membrane. The membrane was blocked in 5% non-fat milk/1 × TTBS (20 mM Tris–HCl, pH 7.5, 150 mM NaCl and 0.05% Tween-20) overnight at 4°C, followed by incubation with anti-hTERT goat polyclonal antibody L-20 (Santa Cruz Biotechnology) in 5% non-fat milk/1 × TTBS for 1 h at room temperature. The membrane was washed three times with 1 × TTBS, then incubated with the HRP-conjugated anti-goat secondary antibody (Santa Cruz Biotechnology) in 5% non-fat milk/1 × TTBS for 1 h at room temperature. The membrane was washed three times with 1 × TTBS, then developed using the Immobilon Western Chemiluminescent HRP substrate (Millipore) following the manufacturer's instructions, and imaged using a Gel Logic440 system (Kodak).

Northern blotting

RNA was extracted from immuno-purified *in vivo* reconstituted telomerase complex by phenol/chloroform extraction and then ethanol precipitated. The extracted RNA was resolved on a 4% polyacrylamide/8 M urea denaturing gel, electrotransferred and UV crosslinked to a Hybond-XL membrane (GE Healthcare). Preparation of the hTR-specific riboprobe and hybridization of the blot were carried out as previously described (Xie *et al*, 2010).

Conventional telomerase activity assay

Telomerase activity assay was carried out as previously described with minor modifications (Xie *et al*, 2010). In brief, 2–3 μl of *in vitro* reconstituted telomerase was assayed in a 10-μl reaction containing 1 × telomerase reaction buffer, 1 mM dTTP, 1 mM dATP, 2 μM dGTP, 0.165 μM α-^{32}P-dGTP (3000 Ci/mmol, 10 mCi/ml, Perkin-Elmer) and 1 μM $(TTAGGG)_3$ DNA primer. The reaction was incubated at 30°C for 60 min and terminated by phenol/chloroform extraction followed by ethanol precipitation. The product was analysed on a 10% polyacrylamide/8 M urea denaturing gel, and the dried gel was analysed using a Bio-Rad FX-Pro phosphorimager.

Template-free telomerase activity assay

The template-free telomerase assay was carried out under a condition similar to the conventional telomerase assay, amended with 20 μM RNA/DNA hybrid as the substrate. The reaction typically contained 0.165 μM α-^{32}P-dGTP (3000 Ci/mmol, 10 mCi/ml, Perkin-Elmer) and 100 μM dTTP if included. The reaction was incubated for 60 min at 4°C or room temperature depending on the T_m of the duplex. The extended products were resolved on an 18% polyacrylamide/8 M urea denaturing gel. For duplex-substrate K_m measurement, the reactions were incubated at 4°C for 30 min with substrate concentrations varying from 0 to 125 μM. For enzyme turnover rate measurement, template-free telomerase was incubated with 20 μM duplex substrate at room temperature for 10 min followed by 4°C for 20 min to ensure saturated enzyme–substrate binding. Equal volume of 0.33 μM α-^{32}P-dGTP in 1 × reaction buffer was pre-chilled on ice and added to initiate nucleotide addition. Reactions were terminated at specific time points by phenol/chloroform extraction followed by ethanol precipitation. The products were analysed by 18% PAGE. Relative turnover rates were determined by the slope of the plotted data points.

Single-translocation assay

Immuno-purified telomerase reconstituted *in vitro* from N-FLAG-hTERT, hTR32-195 (pseudoknot PK-1) and hTR 239-328 (CR4/5) was incubated with 0.2 μM telomeric DNA primer 5′-TT$(AGGGTT)_3$-3′ in 1 × low-Mg^{2+} telomerase reaction buffer (50 mM Tris–HCl pH 8.3, 50 mM KCl, 2 mM DTT, 1 mM $MgCl_2$ and 1 mM spermidine) at room temperature for 10 min and then on ice for 1 min. The single-translocation reaction was initiated by adding 20 μl of incubated enzyme–primer mixture and 20 μl of pre-chilled nucleotide mixture containing 2 mM dATP, 4 μM dGTP, 0.66 μM α-^{32}P-dGTP (3000 Ci/mmol, 10 mCi/ml, Perkin-Elmer) and 2 μM competitive DNA primer 5′-$(TTAGGG)_3$-3′-amine in 1 × low-Mg^{2+} telomerase reaction buffer. Reaction was carried out on ice to slow down enzyme kinetics. Reactions were terminated at specific time points (2, 60, 90 and 120 min) by phenol/chloroform extraction, followed by ethanol precipitation. The products were analysed by PAGE.

Pulse and chase/challenge time-course assay

A 2.5 μl enzyme–primer binding reaction containing 1 μl of *in vivo* reconstituted native template-containing telomerase

and 1 μM DNA primer $(TTAGGG)_3$ in 1 × telomerase reaction buffer was incubated at room temperature for 10 min followed by 4°C for 20 min. The pulse reaction was initiated by adding 2.9 μl of pre-chilled nucleotide mix containing 2 mM dTTP, 2 mM dATP, 4 μM dGTP, 0.33 μM α-^{32}P-dGTP (3000 Ci/mmol, 10 mCi/ml, Perkin-Elmer) in 1 × telomerase reaction buffer. The pulsed reaction was incubated at 4°C for 15 min followed by a chase reaction at 4°C for 90 min. The chase reaction was initiated by adding 4.6 μl of dGTP and competitor mixture. At a final volume of 10 μl, the chase reaction mixture contains 100 μM of non-radioactive dGTP and 200 μM of competitor (5 or 7 bp RNA/DNA duplex or single-stranded oligos). The reaction was terminated by phenol/chloroform extraction, followed by ethanol precipitation and PAGE analysis.

Supplementary data
Supplementary data are available at *The EMBO Journal* Online (http://www.embojournal.org).

Acknowledgements

We thank Dr Tom Cech for providing human POT1 protein and the expression plasmid for human TPP1. We also thank Dr Doug Turner for assistance on predicting the off rate of RNA/DNA hybrids. This work was supported by National Science Foundation Career Award MCB0642857 and National Institutes of Health Grant R01GM094450 to JJLC.

Author contributions: JJLC designed the project and wrote the manuscript. XQ, MX and JJLC designed the experiments. XQ performed the telomerase *in vivo* reconstitution and the single-translocation assay. MX and AFB performed the duplex substrate telomerase assay. AFB performed the POT1–TPP1 telomerase assay. CJB and AFB purified POT1 and TPP1 protein. JDP helped with the manuscript preparation.

Conflict of interest

The authors declare that they have no conflict of interest.

References

Armanios M (2009) Syndromes of telomere shortening. *Annu Rev Genomics Hum Genet* **10:** 45–61

Autexier C, Lue NF (2006) The structure and function of telomerase reverse transcriptase. *Annu Rev Biochem* **75:** 493–517

Bryan TM, Goodrich KJ, Cech TR (2000) Telomerase RNA bound by protein motifs specific to telomerase reverse transcriptase. *Mol Cell* **6:** 493–499

Chen J-L, Blasco MA, Greider CW (2000) Secondary structure of vertebrate telomerase RNA. *Cell* **100:** 503–514

Chen J-L, Greider CW (2003) Determinants in mammalian telomerase RNA that mediate enzyme processivity and cross-species incompatibility. *EMBO J* **22:** 304–314

Chen J-L, Opperman KK, Greider CW (2002) A critical stem-loop structure in the CR4-CR5 domain of mammalian telomerase RNA. *Nucleic Acids Res* **30:** 592–597

Collins K (2008) Physiological assembly and activity of human telomerase complexes. *Mech Ageing Dev* **129:** 91–98

Cristofari G, Adolf E, Reichenbach P, Sikora K, Terns RM, Terns MP, Lingner J (2007) Human telomerase RNA accumulation in Cajal bodies facilitates telomerase recruitment to telomeres and telomere elongation. *Mol Cell* **27:** 882–889

Cristofari G, Lingner J (2006) Telomere length homeostasis requires that telomerase levels are limiting. *EMBO J* **25:** 565–574

Curcio MJ, Belfort M (2007) The beginning of the end: links between ancient retroelements and modern telomerases. *Proc Natl Acad Sci USA* **104:** 9107–9108

Finger SN, Bryan TM (2008) Multiple DNA-binding sites in Tetrahymena telomerase. *Nucleic Acids Res* **36:** 1260–1272

Forstemann K, Lingner J (2005) Telomerase limits the extent of base pairing between template RNA and telomeric DNA. *EMBO Rep* **6:** 361–366

Gillis AJ, Schuller AP, Skordalakes E (2008) Structure of the Tribolium castaneum telomerase catalytic subunit TERT. *Nature* **455:** 633–637

Greider CW (1991) Telomerase is processive. *Mol Cell Biol* **11:** 4572–4580

Huard S, Moriarty TJ, Autexier C (2003) The C terminus of the human telomerase reverse transcriptase is a determinant of enzyme processivity. *Nucleic Acids Res* **31:** 4059–4070

Jacobs SA, Podell ER, Cech TR (2006) Crystal structure of the essential N-terminal domain of telomerase reverse transcriptase. *Nat Struct Mol Biol* **13:** 218–225

Latrick CM, Cech TR (2010) POT1-TPP1 enhances telomerase processivity by slowing primer dissociation and aiding translocation. *EMBO J* **29:** 924–933

Lue NF (2004) Adding to the ends: what makes telomerase processive and how important is it? *Bioessays* **26:** 955–962

Lue NF, Bosoy D, Moriarty TJ, Autexier C, Altman B, Leng S (2005) Telomerase can act as a template- and RNA-independent terminal transferase. *Proc Natl Acad Sci USA* **102:** 9778–9783

Miller MC, Collins K (2002) Telomerase recognizes its template by using an adjacent RNA motif. *Proc Natl Acad Sci USA* **99:** 6585–6590

Min B, Collins K (2010) Multiple mechanisms for elongation processivity within the reconstituted tetrahymena telomerase holoenzyme. *J Biol Chem* **285:** 16434–16443

Mitchell JR, Collins K (2000) Human telomerase activation requires two independent interactions between telomerase RNA and telomerase reverse transcriptase. *Mol Cell* **6:** 361–371

Mitchell M, Gillis A, Futahashi M, Fujiwara H, Skordalakes E (2010) Structural basis for telomerase catalytic subunit TERT binding to RNA template and telomeric DNA. *Nat Struct Mol Biol* **17:** 513–518

Moriarty TJ, Huard S, Dupuis S, Autexier C (2002) Functional multimerization of human telomerase requires an RNA interaction domain in the N terminus of the catalytic subunit. *Mol Cell Biol* **22:** 1253–1265

Morin GB (1989) The human telomere terminal transferase enzyme is a ribonucleoprotein that synthesizes TTAGGG repeats. *Cell* **59:** 521–529

Nakamura TM, Cech TR (1998) Reversing time: origin of telomerase. *Cell* **92:** 587–590

Nakamura TM, Morin GB, Chapman KB, Weinrich SL, Andrews WH, Lingner J, Harley CB, Cech TR (1997) Telomerase catalytic subunit homologs from fission yeast and human. *Science* **277:** 955–959

Northrop DB (1998) On the meaning of Km and V/K in enzyme kinetics. *J Chem Educ* **75:** 1153–1157

Peng Y, Mian IS, Lue NF (2001) Analysis of telomerase processivity: mechanistic similarity to HIV-1 reverse transcriptase and role in telomere maintenance. *Mol Cell* **7:** 1201–1211

Qiao F, Cech TR (2008) Triple-helix structure in telomerase RNA contributes to catalysis. *Nat Struct Mol Biol* **15:** 634–640

Robart AR, Collins K (2011) Human telomerase domain interactions capture DNA for TEN domain-dependent processive elongation. *Mol Cell* **42:** 308–318

Shay JW, Keith WN (2008) Targeting telomerase for cancer therapeutics. *Br J Cancer* **98:** 677–683

Sugimoto N, Nakano S, Katoh M, Matsumura A, Nakamuta H, Ohmichi T, Yoneyama M, Sasaki M (1995) Thermodynamic parameters to predict stability of RNA/DNA hybrid duplexes. *Biochemistry* **34:** 11211–11216

Tesmer VM, Ford LP, Holt SE, Frank BC, Yi X, Aisner DL, Ouellette M, Shay JW, Wright WE (1999) Two inactive fragments of the integral RNA cooperate to assemble active telomerase with the human protein catalytic subunit (hTERT) *in vitro*. *Mol Cell Biol* **19:** 6207–6216

Theimer CA, Blois CA, Feigon J (2005) Structure of the human telomerase RNA pseudoknot reveals conserved tertiary interactions essential for function. *Mol Cell* **17:** 671–682

Turner DH (2000) Conformational changes. In *Nucleic Acids: Structure, Properties, and Functions*, Bloomfield VA, Crothers DM, Tinoco I (eds), Chapter 8, pp 259–334. Sausalito, CA: University Science Books

Wang F, Podell ER, Zaug AJ, Yang Y, Baciu P, Cech TR, Lei M (2007) The POT1-TPP1 telomere complex is a telomerase processivity factor. *Nature* **445:** 506–510

Wu W, Jia Z, Liu P, Xie Z, Wei Q (2005) A novel PCR strategy for high-efficiency, automated site-directed mutagenesis. *Nucleic Acids Res* **33:** e110

Wyatt HD, West SC, Beattie TL (2010) InTERTpreting telomerase structure and function. *Nucleic Acids Res* **38:** 5609–5622

Wyatt HDM, Lobb DA, Beattie TL (2007) Characterization of physical and functional anchor site interactions in human telomerase. *Mol Cell Biol* **27:** 3226–3240

Xie M, Podlevsky JD, Qi X, Bley CJ, Chen JJ (2010) A novel motif in telomerase reverse transcriptase regulates telomere repeat addition rate and processivity. *Nucleic Acids Res* **38:** 1982–1996

Zakian VA (2009) The ends have arrived. *Cell* **139:** 1038–1040

Zaug AJ, Podell ER, Nandakumar J, Cech TR (2010) Functional interaction between telomere protein TPP1 and telomerase. *Genes Dev* **24:** 613–622